

Reversibility of Retinal Ganglion Cell Dysfunction From Chronic IOP Elevation

Da Zhao,¹ Vickie H. Y. Wong,¹ Christine T. O. Nguyen,¹ Andrew I. Jobling,² Erica L. Fletcher,² Algis J. Vingrys,¹ and Bang V. Bui¹

¹Department of Optometry and Vision Sciences, University of Melbourne, Parkville, Victoria, Australia

²Department of Anatomy and Neuroscience, University of Melbourne, Parkville, Victoria, Australia

Correspondence: Bang V. Bui, Department of Optometry and Vision Sciences, The University of Melbourne, Parkville, Victoria 3010, Australia; bvb@unimelb.edu.au.

Submitted: March 18, 2019

Accepted: August 13, 2019

Citation: Zhao D, Wong VHY, Nguyen CTO, et al. Reversibility of retinal ganglion cell dysfunction from chronic IOP elevation. *Invest Ophthalmol Vis Sci*. 2019;60:3878–3886. <https://doi.org/10.1167/jovs.19-27113>

PURPOSE. To test the hypothesis that the capacity for retinal ganglion cells to functionally recover from chronic IOP elevation is dependent on the duration of IOP elevation.

METHODS. IOP elevation was induced in one eye in anesthetized (isoflurane) adult C57BL/6J mice using a circumlimbal suture. Sutures were left in place for 8 and 16 weeks ($n = 30$ and 28). In two other groups the suture was cut after 8 and 12 weeks ($n = 30$ and 28), and ganglion cell function (electroretinography) and retinal structure (optical coherence tomography) were assessed 4 weeks later. Ganglion cell density was quantified by counting RBPMS (RNA-binding protein with multiple splicing)-stained cells.

RESULTS. With IOP elevation (~ 10 mm Hg above baseline), ganglion cell function declined to $75\% \pm 8\%$ at 8 weeks and $59\% \pm 4\%$ at 16 weeks relative to contralateral control eyes. The retinal nerve fiber layer was thinner at 8 ($84\% \pm 4\%$) and 16 weeks ($83\% \pm 3\%$), without a significant difference in total retinal thickness. Ganglion cell function recovered with IOP normalization (suture removal) at week 8 ($97\% \pm 7\%$), but not at week 12 ($73\% \pm 6\%$). Ganglion cell loss was found in all groups (-8% to -13%).

CONCLUSIONS. In the mouse circumlimbal suture model, 12 weeks of IOP elevation resulted in irreversible ganglion cell dysfunction, whereas retinal dysfunction was fully reversible after 8 weeks of IOP elevation.

Keywords: ganglion cells, recovery, intraocular pressure, adenosine receptors, electroretinogram

Glaucoma is a group of eye diseases where vision is lost due to progressive damage to retinal ganglion cells (RGCs) and their axons.^{1,2} Increased intraocular pressure (IOP) is currently the only modifiable risk factor.^{3,4} Prompt IOP lowering can prevent further RGC injury^{5,6}; however, in some cases IOP reduction does not prevent vision loss and glaucoma progression.^{5,7–9} It has been generally accepted that IOP-induced RGC injury is irreversible. Indeed, current treatments are largely aimed at halting further disease progression, but it is assumed that visual field loss and retinal nerve fiber layer (RNFL) thinning cannot be restored.^{6,10,11}

Whilst ganglion cell loss is irreversible, there is strong evidence that ganglion cell dysfunction is recoverable. Ventura et al.¹² have shown that an acute mild IOP elevation induced by head down tilt produces attenuation of the pattern electroretinogram (ERG) that is fully reversible with IOP normalization. Laboratory studies also show that short-term high IOP-induced RGC dysfunction is fully reversible.¹³ Indeed, even extended periods of IOP elevation in 4-week-old rats do not lead to irreversible damage, as evidenced by ERG recovery after IOP normalization.¹⁴ Consistent with these findings, recent clinical studies^{11,15–19} report improvements in visual sensitivity in some early glaucoma/ocular hypertensive patients with IOP lowering. As such there is increasing evidence to suggest that RGC dysfunction is recoverable if intervention to normalize IOP occurs early enough, perhaps before some critical time threshold is reached. Whilst acute-IOP studies have attempted

to examine the relationship between the duration of IOP elevation and functional recovery,²⁰ few studies have sought to define the duration of chronic IOP elevation that might lead to irreversible dysfunction. Comparing cellular differences between reversible and irreversible dysfunction has the potential to progress our understanding of glaucoma pathogenesis.

It is established that elevated IOP causes mechanical stress, which leads to remodelling of optic nerve head and peripapillary connective tissues. In addition to changes to axonal transport and vascular supply, IOP elevation can impact RGCs directly by activation of channels that are sensitive to stretching of the cell membrane, which drive cell death through apoptotic mediators.¹⁰ However, before cell death, compensatory cellular adaptations, including axonal transport enhancement, synaptic remodeling, and dendrite shrinkage have been shown to occur.^{21–24} It is likely that these protective mechanisms are overwhelmed when cell loss occurs. Perhaps early on in the sequence of cellular injury, before cell loss, RGCs may retain the capacity to functionally recover.

In addition to recapitulating features of human glaucoma,^{25,26} the circumlimbal suture rodent model of chronic IOP elevation allows IOP to be normalized back to baseline (by removing the suture) at any time without need of pharmacologic agents, which may also have secondary effects. In this study we used the circumlimbal suture model of chronic IOP elevation to test the hypothesis that the duration of IOP



elevation changes the capacity for ganglion cell function to recover with IOP normalization.

METHODS

Animals

Adult C57BL/6 mice (8 weeks old) purchased from the Animal Resources Centre (Canning Vale, WA, Australia) were used in this study. All procedures followed the requirements of the National Health and Medical Research Council of Australia statement for the use of animals in research, the Association for Research in Vision and Ophthalmology (ARVO) Statement for the Use of Animals in Ophthalmic and Vision, and were approved by the Howard Florey Animal Ethics Committee (13-068-UM). Mice were housed with free access to water and normal rodent chow (Barastoc, Melbourne, VIC, Australia) in the Melbourne Brain Centre (Parkville, VIC, Australia). Room temperature was maintained at 21°C, with animals exposed to a 12-hour light/dark cycle (on at 7 AM, <50 lux inside the cage).

All surgical procedures were performed under general anesthesia using isoflurane inhalation (mixture of 1.5% isoflurane balanced with O₂ at a flow rate of 2 L/min, IsoFlo; Abbott, North Chicago, IL, USA). During end point assessment (electroretinography and optical coherence tomography imaging), animals underwent general anesthesia via an intraperitoneal injection of a ketamine and xylazine cocktail (80 and 10 mg/kg; Troy Laboratory, Glendenning, NSW, Australia). Additional topical anesthesia and pupil dilation were achieved with Alcaine (1% proxymetacaine; Alcon Laboratory, Sydney, NSW, Australia) and Mydracil (0.5% tropicamide; Alcon), respectively. To maintain corneal hydration, a lubricating gel (GenTeal; Alcon) was used. Body temperature was maintained whilst under anesthesia at ~37°C by using an electrical heat pad.

IOP Manipulation and Measurement

The circumlimbal suture model in mice has been described in detail previously.²⁶ Briefly, in anesthetized (isoflurane) mice, a 10/0 nylon suture was threaded through the conjunctiva 1 mm posterior to the limbus to induce IOP elevation. At selected time points (either 8 or 12 weeks) IOP was restored back to baseline by placing mice under general anesthesia (isoflurane) and removing the suture by cutting the knot and gently pulling out the residual suture.

In total 150 mice were used in this study (Supplementary Fig. S1); 34 animals (22%) were excluded owing to corneal or anterior segment complications following surgery. A final 116 mice were included in two ocular hypertension (OHT) groups (IOP elevation for 8 and 16 weeks' OHT, $n = 30$ and 28) and two suture cut (SC) groups (suture removal after 8 and 12 weeks of IOP elevation, $n = 30$ and 28). In the SC groups, assessment and tissue collection were undertaken 4 weeks after IOP suture removal. In each animal, one random eye was chosen for surgery to elevate IOP, and the contralateral eye served as control. An extra three groups of age-matched naïve control mice were included (8 weeks, 12 weeks, and 16 weeks, $n = 7$ –8/group) for comparison.

For acclimatization to awake IOP measurement, animals were handled daily for 1 week before the suture implantation. During this week three baseline IOPs were measured over 3 days. IOP was noninvasively measured by using a rebound tonometer (TonoLab; Icare Finland Oy, Vantaa, Finland) in awake mice without corneal anesthesia, except at the 2-minute time point immediately after the surgery, when mice were still under the influence of isoflurane anesthesia. IOP was

measured at 2 minutes and 1 hour after suture implantation; 1 day, 2 day, and 3 days post operation; and then weekly thereafter. To minimize diurnal fluctuations, IOP measurements were performed around 10:00 AM, and 10 measurements were taken for each eye and averaged.

Electroretinography

Retinal function was examined by using scotopic full-field ERG described previously.²⁷ Animals were dark-adapted overnight before recording to achieve maximal retinal sensitivity. Mice underwent general anesthesia (ketamine and xylazine) with additional corneal anesthesia (1% proxymetacaine; Alcon) and mydriasis (0.5% tropicamide; Alcon) before placement on a platform warmed with circulating water for electrode placement. Pairs of custom-made silver electrodes (99.9% silver; A&E Metal Merchants, Sydney, NSW, Australia) were used; on each eye an active electrode and a ring-shaped inactive electrode were placed on the apex of the cornea and the equator of the sclera, respectively. A stainless-steel needle electrode was inserted into the tail to serve as the ground (F-E2-30; Grass Telefactor, West Warwick, RI, USA).

ERGs were recorded using Scope software (ADInstruments Pty Ltd., Bella Vista, NSW, Australia) as described previously.^{26,28} A series of gradually increasing luminous exposures were delivered via a precalibrated LED light source integrated into a Ganzfeld sphere (Photometric Solutions International, Oakleigh, VIC, Australia). Light energies ranging from -6.53 to $2.07 \log \text{cd}\cdot\text{s}/\text{m}^2$ were delivered to examine signals from a range of different retinal cell classes. Photoreceptor function was modelled using a delayed-Gaussian function to expose the maximal amplitude (RmP3).²⁹ Bipolar cell function was quantified using a Naka Rushton function to model the P2 amplitude (raw ERG - P3) as a function of luminous exposure, to return the maximum amplitude (Vmax).³⁰ RGC function was measured as the peak amplitude of the positive scotopic threshold response (pSTR) at both 5.01 and $-4.90 \log \text{cd}\cdot\text{s}/\text{m}^2$.^{31–33}

Optical Coherence Tomography

Following ERG recording, retinal structure and blood flow was imaged using spectral-domain optical coherence tomography (SD-OCT, Envisu R2200 VHR; Biophtigen, Inc., Wetzlar, Germany), as described previously.²⁶ Briefly, two customized lenses for rodents were used to capture the anterior (18-mm telecentric lens; Biophtigen) and posterior (rat posterior lens; Biophtigen) segments, respectively. The anesthetized mouse was placed on a three-dimensional alignment stage and was kept warm by using a rodent heat pad. The pupil was well dilated (as above) and a drop of corneal lubricant (Systane; Alcon Laboratories, Fort Worth, TX, USA) was applied to obtain clear optics.

Anterior segment imaging used a 4×4 -mm scan (100 B-scans, 1000 A-scan/B-scan), and the posterior segment centered around the optic nerve head was imaged with a 2.5×2.5 -mm volume scan (200 B-scans, 1000 A-scan/B-scan). Following structural OCT, an annular Doppler blood flow B-scan (in total 1000 A-scans) around the optic nerve head was taken to quantify retinal blood flow. Detectable real-time Doppler signal shift induced by flow was indicated by red (arterial flow, toward the objective) and blue (venous flow, away from the objective) pixels.

Images acquired from the Biophtigen OCT were processed and analyzed by using Fiji software (<https://fiji.sc/>; provided in the public domain). A horizontal B-scan through the center of the cornea was used to measure the trabecular meshwork-iris angle in both eyes. Pupil size was determined by the average of

horizontal (180°) and vertical (90°) width from the en face image. To assay differences in retinal structure, 3 to 5 horizontal B-scans crossing the optic nerve head were averaged for manual segmentation. In each eye, the boundaries of the inner limiting membrane, RNFL, inner plexiform layer (IPL), and Bruch's membrane were manually segmented in a masked fashion. The thickness of each layer and the total retinal thickness (TRT) was returned by averaging both temporal and nasal regions at 200 μm to 400 μm from the center of the Bruch's membrane opening. Retinal blood flow was assayed by counting the number of red and blue pixels, using FIJI (<https://fiji.sc/>), in the prethresholded Doppler blood flow images.

Histology

After ERG recording and OCT imaging, a subset of mice from each group ($n = 12$ –16) was allocated to retinal histology as described previously.²⁶ RGCs were stained by RNA-binding protein with multiple splicing (RBPMS, 1:1000, rabbit, polyclonal; Invitrogen, Thermo Fisher Scientific, Carlsbad, CA, USA), which has been shown to be a highly specific marker of ganglion cells in rodents,³⁴ with goat anti-rabbit Alexa Fluor 647 (1:500; Invitrogen) and Hoechst (1:1000, 10 minutes, room temperature; Roche Applied Science, Penzberg, Upper Bavaria, Germany). The retina was then orientated and flat-mounted with Mowiol (Sigma-Aldrich, Darmstadt, Germany). Confocal images were acquired with a Leica SP8 confocal microscope ($\times 40$, oil; Leica Microsystems, Wetzlar, Germany) from eight retinal regions: both central and peripheral areas in all quadrants (superior, temporal, nasal, and inferior). In each region a Z-series through the RGC layer was scanned at 1- μm steps by using a 512×512 -pixel window ($290.62 \times 290.62 \mu\text{m}$). The Z-stack was averaged to return the maximum intensity, and the RPBMS channel and Hoechst channel were composited to confirm the existence of ganglion cells. RGCs were manually counted in a masked fashion by using FIJI software.

Statistical Analysis

Statistical analysis was performed with Prism 8 software (GraphPad Software, Inc., San Diego, CA, USA). Outlier analysis was undertaken on all data sets using ROUT analysis test. Two animals in separate groups were removed from all analyses. Group data are expressed as mean \pm standard error of the mean (SEM), and the treated eyes were also plotted as a percentage of their own untreated contralateral control. Paired *t*-tests (treated versus control), 1-way ANOVAs, and 2-way ANOVAs were conducted as appropriate. Tukey's test was used for post hoc multiple comparison.

RESULTS

Before the induction of OHT, baseline IOP was similar between treated and control eyes in all groups (~ 15 –18 mm Hg, all $P > 0.05$). Figures 1A and 1B show the IOP profiles in the two OHT groups (8 weeks and 16 weeks of IOP elevation, 8wk-OHT and 16wk-OHT) and the two SC groups (the suture was removed at weeks 8 and 12 and assessment was undertaken 4 weeks later, 8wk-SC and 12wk-SC), respectively. As previously shown,²⁶ a mild IOP spike was evident immediately after suturing (~ 40 –50 mm Hg) in all groups, that returned to 30 mm Hg by day 3 (Fig. 1C). IOP was sustained between 25 and 30 mm Hg in sutured eyes throughout the 8 to 16 weeks of the study (Fig. 1). In the OHT groups, IOP in treated eyes was significantly increased (8wk-OHT: 26.8 ± 0.6 vs. 17.1 ± 0.3 mm Hg, $P < 0.001$; 16wk-OHT: 27.4 ± 0.6 vs. 17.0 ± 0.2 mm Hg, $P <$

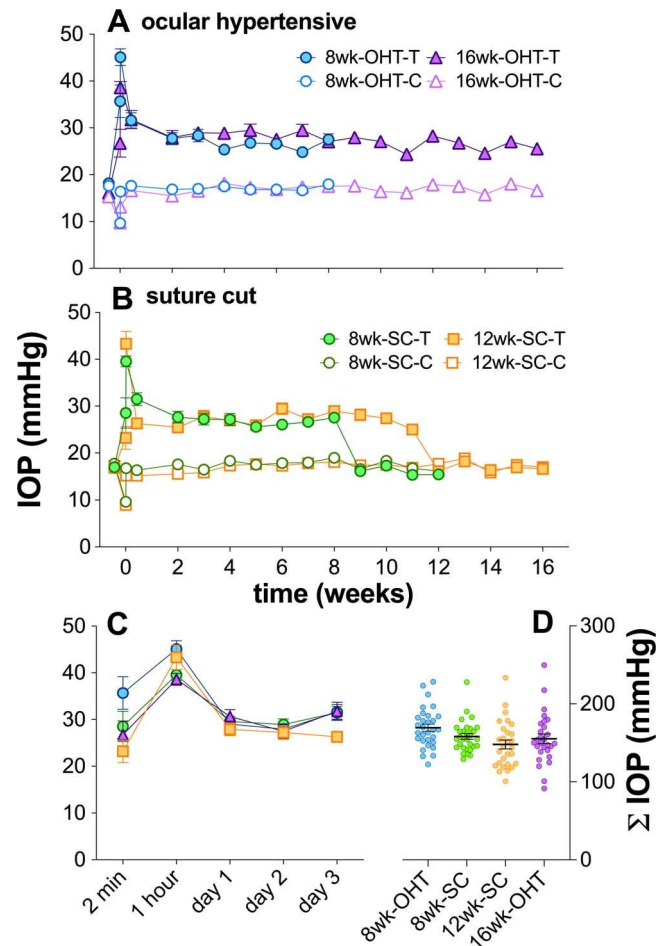


FIGURE 1. IOP elevation in mouse eyes, induced by circumlimbal suture. (A) Average (\pm SEM) IOP of treated (filled symbols) and control (unfilled symbols) eyes for 8-week (8wk-OHT, circles, $n = 30$) and 16-week ocular hypertensive (16wk-OHT, triangles, $n = 28$) groups. (B) IOP was increased when the suture was in place and was normalized after suture removal in the 8-week suture cut (8wk-SC, $n = 30$, filled circles) and 12-week suture cut (12wk-SC, $n = 28$, filled squares) groups. (C) Average (\pm SEM) IOP at 2 minutes, 1 hour, and during the first 3 days in treated eyes from all groups. (D) Summed IOP over the five measurement points shown in (C). Data for all treated eyes are plotted with group average (\pm SEM).

0.001, average of week 2 until the end; Fig. 1A), as well as in the SC groups (8wk-SC: 26.8 ± 0.6 vs. 17.8 ± 0.3 mm Hg, $P < 0.001$; 12wk-SC: 26.2 ± 0.6 vs. 17.1 ± 0.2 mm Hg, $P < 0.001$; Fig. 1B). The magnitude of IOP elevation in treated eyes was comparable between groups (8wk-OHT: 9.7 ± 0.6 mm Hg, 16wk-OHT: 10.4 ± 0.6 mm Hg, 8wk-SC: 9.0 ± 0.5 mm Hg, 12wk-SC: 9.0 ± 0.6 mm Hg, $P < 0.001$). Suture removal restored IOP back to levels comparable to control eyes (8wk-SC: 16.0 ± 0.3 vs. 16.9 ± 0.3 mm Hg, $P = 0.08$; 12wk-SC: 17.0 ± 0.3 vs. 17.3 ± 0.2 mm Hg, $P = 0.49$).

During the first 3 days there was no difference between the IOP profile of treated eyes between the 8wk-OHT and the 8wk-SC group (2-way ANOVA, $F_{1,290} = 3.4$, $P = 0.07$; Fig. 1C). However, early IOPs were significantly higher in the 8wk-OHT group than in both the 12wk-SC group ($F_{1,280} = 11.8$, $P < 0.001$) and the 16wk-OHT group ($F_{1,280} = 5.1$, $P = 0.03$). IOP was also summed over the first five measurement points (2 minutes to 3 days) as shown in Figure 1D. One-way ANOVA showed that there was a significant difference between groups ($F_{11,112} = 3.1$, $P = 0.03$). Post hoc analysis indicated that

summed IOP in the 8wk-OHT group was significantly higher than in the 12wk-SC group, but not the other groups.

At selected end points all animals underwent functional assessment with scotopic full-field ERG, the outcomes of which are summarized in Figure 2. Figures 2A and 2B show the averaged ERG waveforms for control and treated eyes from animals that had undergone 8 or 12 weeks of IOP elevation before suture removal, respectively. As shown in Figure 2A, after 4 weeks of recovery following 8 weeks of chronic IOP elevation (8wk-SC) ganglion cell function (pSTR) in treated eyes (green trace) was similar to responses recorded from contralateral control eyes (gray trace). In contrast, Figure 2B shows that after 4 weeks of recovery from 12 weeks of chronic IOP elevation (12wk-SC) ganglion cell responses (orange trace) had not recovered, as evidenced by the attenuation of the STR when compared with control eyes (gray trace). Differences in photoreceptor and bipolar cell waveforms between control and treated eyes were less obvious in the two SC groups (upper row of Figs. 2A, 2B).

Individual amplitudes for photoreceptor (Rmp3), bipolar cell (Vmax), and ganglion cell (pSTR) function are plotted for control and treated eyes in Figures 2C through 2E. Retinal dysfunction was evident across photoreceptor ($78.6\% \pm 4.8\%$ of controls, $P < 0.001$; Fig. 2C), bipolar cell ($76.7\% \pm 4.6\%$ of controls, $P < 0.001$; Fig. 2D), and ganglion cell ($77.2\% \pm 7.5\%$ of controls, $P = 0.0014$; Fig. 2E) responses after 8 weeks of IOP elevation (8wk-OHT). By 16 weeks of IOP elevation, ganglion cell dysfunction appeared to have progressed (16wk-OHT: $58.9\% \pm 4.2\%$, $P = 0.035$ versus 8wk-OHT), whereas there was no further attenuation of bipolar cell (16wk-OHT: $80.7\% \pm 4.8\%$, $P = 0.55$ versus 8wk-OHT) and photoreceptor function (16wk-OHT: $79.2\% \pm 4.9\%$, $P = 0.93$ versus 8wk-OHT).

In the 8-week SC group (8wk-SC) amplitudes for ERG components of treated eyes were not significantly different from those of contralateral control eyes (photoreceptor: $95.8\% \pm 3.6\%$ of controls, $P = 0.15$; bipolar cell: $95.5\% \pm 4.4\%$, $P = 0.1$; ganglion cell: $96.7\% \pm 7.1\%$, $P = 0.21$). In contrast to the recovery seen in the 8-week SC group, amplitudes for all ERG components in the 12-week SC (12wk-SC) group were significantly smaller than those of their contralateral control eyes (photoreceptors: $89.5\% \pm 5.2\%$ of controls, $P < 0.001$; bipolar cell: $89.3\% \pm 5.2\%$, $P = 0.001$; ganglion cell: $72.5\% \pm 6.3\%$, $P = 0.009$, of controls). This would indicate that there was no or incomplete recovery of function in the 12-week SC group. In summary, when the suture was cut at 8 weeks, retinal function recovered close to baseline levels. In contrast, with a longer period of IOP elevation (12 weeks) retinal function was unable to recover, indicating that 12 weeks is a critical duration for irreversible IOP-induced neuron injury in this model.

Grouped average retinal layer thicknesses are shown in Figures 3A through 3C. There was no significant difference in IPL (Fig. 3B) and TRT (Fig. 3C); however, RNFL thickness (Fig. 3A) was significantly reduced in treated eyes compared to their own control eyes in all OHT groups (8wk-OHT: 18.4 ± 0.8 vs. 22.2 ± 0.8 μm , $P < 0.001$; 16wk-OHT: 15.2 ± 0.6 vs. 18.7 ± 0.9 μm , $P < 0.001$). The RNFL was 12% to 18% thinner in all groups, with no significant differences between groups (1-way ANOVA, $P = 0.619$). Similar magnitudes of RNFL thinning were also observed in both 8wk-SC and 12wk-SC groups (8wk-SC: 17.7 ± 0.6 versus control 20.8 ± 0.8 μm , $P < 0.001$; 12wk-SC: 16.7 ± 0.6 versus control 19.1 ± 0.8 μm , $P = 0.001$). OCT assessment of anterior segments including pupil size and trabecular meshwork-iris angle did not reveal any differences between groups (see Supplementary Fig. S2). Also, there was no significant difference in retinal blood flow assayed with Doppler OCT between groups (see Supplementary Fig. S2).

Retinal tissue from half of the mice from each group was collected for histologic assessment. Figure 4 shows the results of flat-mount RGC counts in four quadrants. As shown in Figures 4A and 4B, there were fewer RGCs (red, stained by RBPMS) present in treated eyes than in control eyes for superior ($91.5\% \pm 3.1\%$) and nasal quadrants ($92.4\% \pm 3.3\%$), after 8 weeks of ocular hypertension (temporal: $95.1\% \pm 3.0\%$; inferior: $94.0\% \pm 3.3\%$). RGC loss was greatest in the 16wk-OHT group with all quadrants being significant (superior: $87.8\% \pm 2.4\%$; nasal: $92.2\% \pm 2.6\%$; inferior: $90.6\% \pm 2.9\%$; temporal: $89.7\% \pm 2.3\%$). In the 8-week SC groups all quadrants (superior: $90.9\% \pm 2.3\%$; nasal: $94.5\% \pm 1.8\%$; inferior: $92.7\% \pm 2.5\%$) with the exception of the temporal ($95.6\% \pm 3.5\%$) segment showed significantly reduced ganglion cell density. However, comparisons across groups show that there were no significant differences (1-way ANOVA, superior: $P = 0.691$, nasal: $P = 0.947$, inferior: $P = 0.876$, temporal: $P = 0.382$). In summary, all groups (OHT and SC) exhibited a loss of RGCs across most quadrants; however, the duration of IOP injury and IOP normalization did not appear to alter the severity of RGC loss (Figs. 4B–E), or RNFL thinning (Fig. 3).

DISCUSSION

This is the first study to show, in a murine model that can repeatably control the duration of IOP elevation, that there is a critical duration (12 weeks) for IOP elevation beyond which retinal function is irreversibly lost. A duration of 8 weeks afforded complete functional recovery. It corroborates and builds upon a previous longitudinal study conducted in rats³⁵ that shows that 8 weeks of chronic IOP elevation causes retinal dysfunction, which can be ameliorated if the pressure is normalized at this point. The current study illustrates that functional recovery from 8 weeks of chronic IOP elevation is repeatable in a mouse model; however, it goes further in showing that 12 weeks of IOP elevation results in irreversible injury.

The circumlimbal suture model in this study induced a sustained elevation of IOP to ~ 25 to 27 mm Hg, a level that is consistent with other rodent glaucoma models including those using intracameral microbead injection, episcleral hypertonic saline injection, laser photocoagulation, and episcleral vein ligation.^{36–40} However, it is worth noting that our IOP measurements were taken in awake mice, whereas most previous studies take readings in anesthetized animals. As awake IOPs can be higher than anesthetized readings, our levels of IOP-induced stress may be lower than previous studies.

A single surgical intervention induced sustained stable IOP elevation even up to 16 weeks, which was the longest end point assayed in this study. Although an IOP spike occurred immediately after suture implantation, the long-term effect has been shown to be negligible.^{26,35} Furthermore, the sham surgical procedure, in which the suture was implanted but IOP not elevated, produced no functional or anatomical changes.²⁵ Figures 1C and 1D show that the IOP profile during the first 3 days was similar between all groups. Removal of the suture provides the opportunity to simulate treatment (IOP lowering) in the clinic without introducing pharmacologic agents.

Retinal function as assessed with ERG showed that ganglion cells were more affected by OHT between 8 and 16 weeks of chronic IOP elevation than photoreceptors and bipolar cells (Figs. 2C, 2D). This preferential progression of ganglion cell dysfunction with longer periods of IOP elevation has also been noted in the rat circumlimbal suture model,²⁵ mouse circumlimbal suture model,^{35,41} as well as the DBA2J mouse.⁴²

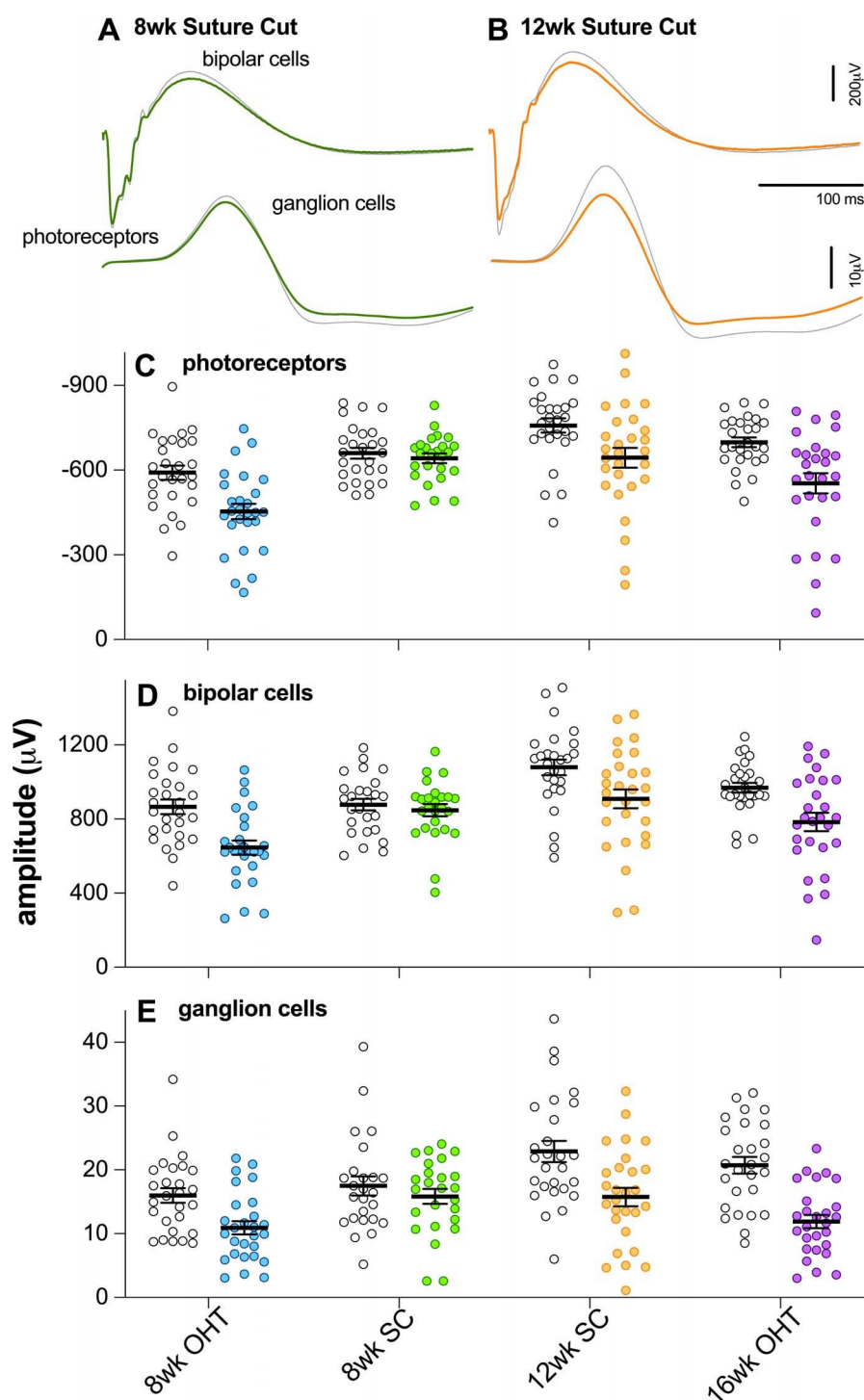


FIGURE 2. Effect of chronic IOP elevation and its reversal on retinal function. (A, B) Grouped average ERG waveforms elicited with a bright ($2.07 \log \text{cd-s/m}^2$, indicative of photoreceptor and bipolar cell function) and dim ($-4.9 \log \text{cd-s/m}^2$, ganglion cell function) flash for control (grayed trace) and treated (colored traces) in the 8-week suture cut (8wk-SC, green traces) and 12-week suture cut (12wk-SC, orange traces) groups. (C) Comparison of photoreceptor amplitudes (RmP3) for all control (unfilled symbols) and treated (colored symbols) eyes from 8-week ocular hypertensive (8wk-OHT, $n = 27$), 8-week suture cut (8wk-SC, $n = 26$), 12-week suture cut (12wk-SC, $n = 27$), and 16-week ocular hypertensive (16wk-OHT, $n = 27$) groups, along with group average ($\pm \text{SEM}$). (D) Comparison of bipolar cell amplitudes (Vmax) for control and treated eyes from 8wk-OHT, 8wk-SC, 12wk-SC, and 16wk-OHT groups. (E) Comparison of ganglion cell amplitudes (pSTR) for control and treated eyes from 8wk-OHT, 8wk-SC, 12wk-SC, and 16wk-OHT groups. * $P < 0.05$, ** $P < 0.01$, *** $P < 0.001$.

The data also suggest that there is variability in the contralateral control eye responses between groups (Fig. 2), which can in part be accounted for by aging effects. More specifically, age-matched naïve control eyes (Supplementary

Fig. S3) showed that the ERG response grows between 18 and 24 weeks and declines somewhat between 24 and 30 weeks of age. Maturation of the murine ERG response has previously been reported to occur up to 12 weeks of age, thereafter

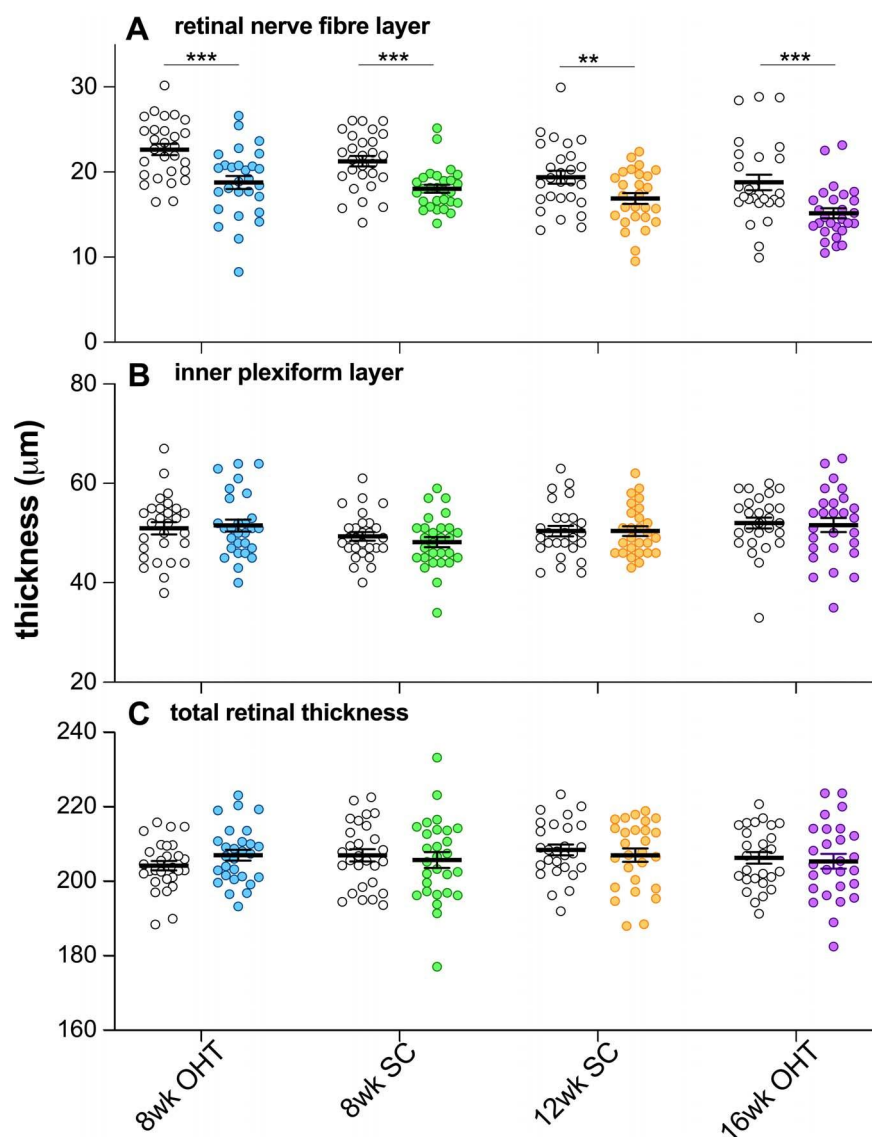


FIGURE 3. Effect of IOP elevation and its reversal on retinal structure. (A) Comparison of RNFL thickness for all treated (colored symbols) and control (unfilled symbols) eyes in 8-week ocular hypertensive (8wk-OHT, $n = 28$), 8-week suture cut (8wk-SC, $n = 28$), 12-week suture cut (12wk-SC, $n = 27$), and 16-week ocular hypertensive (16wk-OHT, $n = 27$) groups, along with group average (\pm SEM). (B) Comparison of IPL thickness between treated and control eyes in 8wk-OHT, 8wk-SC, 12wk-SC, and 16wk-OHT groups. (C) Comparison of TRT between treated and control eyes in 8wk-OHT, 8wk-SC, 12wk-SC, and 16wk-OHT groups. ** $P < 0.01$, *** $P < 0.001$.

declining at 24 and 48 weeks of age.⁴³ These data illustrate the importance of age-matched controls. An important consideration with using the contralateral eye as a control is the possibility that this is also impacted by IOP elevation.⁴⁴ Supplementary Figure S3 suggests that there is a trend for contralateral control eyes to return smaller amplitudes than those of age-matched naive controls; however, these differences were not significant.

Retinal dysfunction was associated with RNFL thinning and ganglion cell loss (Figs. 3, 4), but interestingly without significant IPL thinning. Previous studies have noted that ocular hypertension in mice results in more RNFL and ganglion cell layer thinning than in IPL attenuation.⁴⁵ Thus RNFL change may precede IPL changes in mouse models of ocular hypertension. Alternatively, IOP-induced microglial reactivity in the IPL may mask ganglion cell dendritic changes.⁴⁴

It is of interest that ganglion cell dysfunction progressed but structural measures such as RNFL thickness and RGC cell

density did not significantly decrease between 8 and 16 weeks of IOP injury. Although there was a further 3% decline in RGC density, (8wk-OHT: $93.2\% \pm 1.1\%$, 16wk-OHT: $90.1\% \pm 1.7\%$, $P = 0.12$), this is unlikely to account for the drop of ganglion cell function from 77.2% after 8 weeks of IOP elevation to 58.9% after 16 weeks of injury. It is possible that as RBPMS does not stain all RGCs,³⁴ progression of cell loss occurred but was not detectable with this particular stain. Others have reported that IOP-induced reductions in the pSTR can be greater than RGC cell loss,^{46,47} which would suggest that the presence of IOP elevation attenuates the pSTR response. Studies showing that acute IOP elevation induce reversible STR attenuation, where cell loss is not a factor, support this idea.^{20,48} The current data showed that between 8 and 16 weeks of chronic IOP elevation, the density of RBPMS-stained cells is the same but that their light responses are further attenuated. This finding might indicate that progression of pSTR attenuation involves mechanisms independent of further

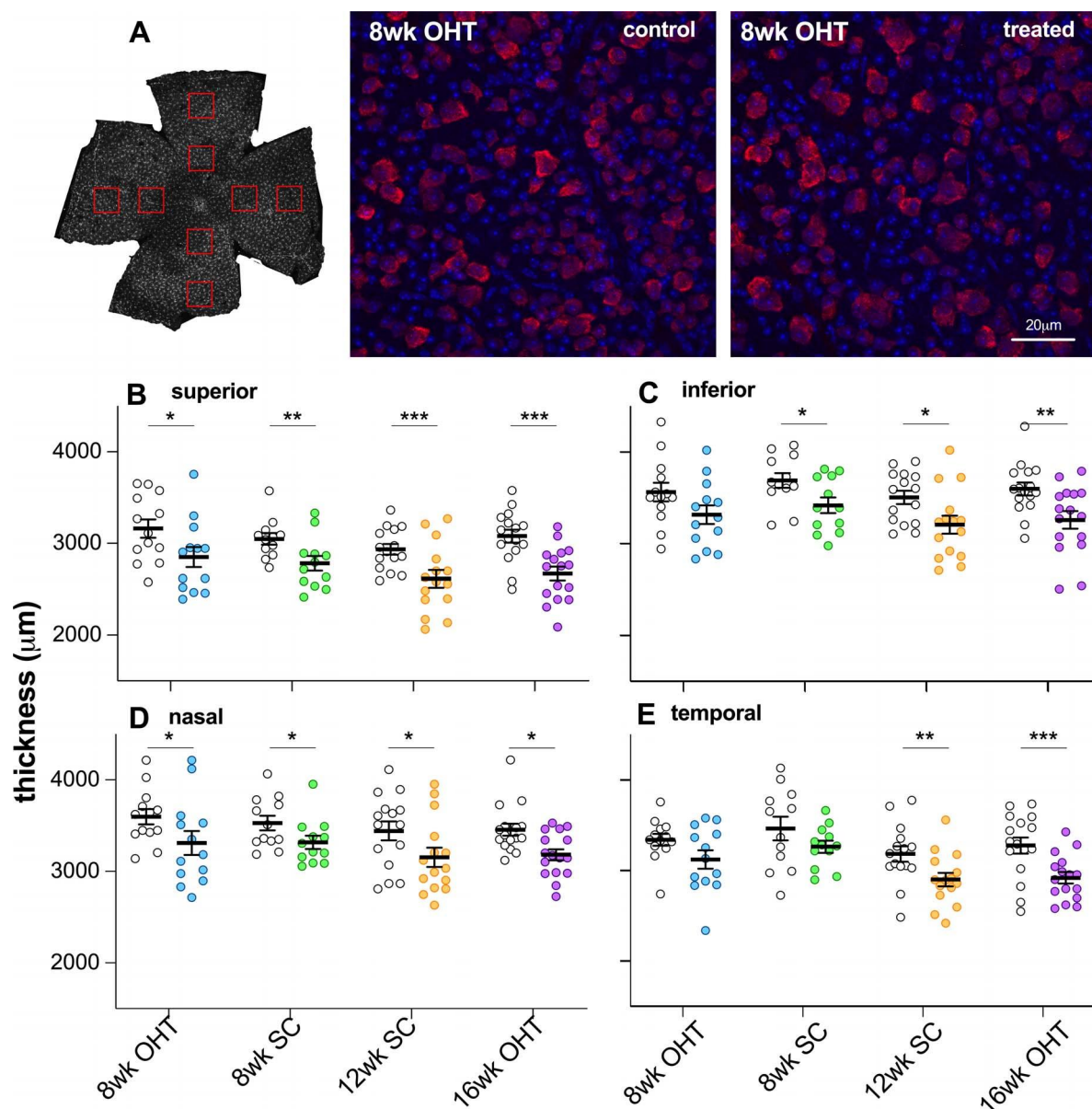


FIGURE 4. Effect of IOP elevation and its reversal on retinal ganglion cell density. (A) Retina flat-mount images with RGC specific staining (red: RBPMS, ganglion cells; blue: Hoechst, nuclei) of a sutured and control eye from the same animal in the 8-week ocular hypertensive (8wk-OHT) group. (B) Comparison of RGC density in the superior retina for all control (gray violin plots) and treated (colored violin plots) eyes for 8-week ocular hypertensive (8wk-OHT, green, $n = 13$), 8-week suture cut (8wk-SC, green dotted, $n = 12$), 12-week suture cut (12wk-SC, orange, $n = 15$), and 16-week ocular hypertensive (16wk-OHT, purple, $n = 16$) groups, along with group average (\pm SEM). (C) Comparison of RGC density in the inferior quadrant for all control and treated eyes in 8wk-OHT, 8wk-SC, 12wk-SC, and 16wk-OHT groups. (D) Comparison of RGC density in the nasal retina. (E) Comparison of RGC density in the temporal retina. * $P < 0.05$, ** $P < 0.01$, *** $P < 0.001$.

RGC loss. Greater pSTR attenuation was also independent of reduced upstream input, as we saw no further reduction of photoreceptor or bipolar cell responses when comparing 8 and 16 weeks of OHT.

We found a clear difference in the capacity for functional recovery between 8 and 12 weeks of IOP elevation. Improved function in the 8wk-SC group did not arise because of a difference in the IOP profile, as acute (Figs. 1C, 1D) and chronic (Fig. 1A) IOPs were not different between the 8wk-SC and any of the other groups. It is important to note that the absence of recovery we observed at 12 weeks was only assessed at a single time point, 4 weeks after IOP normalization (suture cut). It may be that functional recovery is possible but takes longer than 4 weeks. For short periods of acute IOP

elevation, higher magnitude and longer duration of IOP elevation result in slower functional recovery.²⁰

The mechanisms underlying functional recovery we observed in the 8wk-SC group require investigation. As might be expected, structurally there was very little difference between the 8-week high-IOP group and the 8-week SC group in terms of retinal layer thicknesses measured with OCT and RGC cell density. Recovery of neuronal function might therefore reflect an upregulation of output from the remaining retinal neurons. This can happen in two ways. Firstly, the recovery of photoreceptor (a-wave) and bipolar cell function (b-wave) as seen in the 8-week SC group will increase input to downstream ganglion cells, thus leading to improved pSTR amplitudes.⁴⁹

However, outer retinal responses only returned to normal levels, comparable to control eyes; therefore, some compensatory change in the inner retina or in ganglion cells would still have been required to maintain pSTR amplitude at normal levels despite the RGC loss in the 8wk-SC group.

Suture removal will ameliorate IOP-related stressors, which can dampen the neuronal activity of remaining neurons. IOP elevation acts on channels sensitive to stretching, including transient receptor potential (vanilloid)^{50–52} and purinergic receptors,^{53,54} which are known to modulate ionic movements across the cell membrane in retinal neurons including ganglion cells. Removal of IOP-related activation of such channels can impact neuronal responses to light and thus the ERG. Stretch-sensitive receptors are found both in the outer and inner retina,^{50,53} which may account for our observation that both inner and outer and retinal responses showed recovery with IOP lowering. The exact mechanism mediating restoration of function warrants further investigation.

In summary, in a mouse model of OHT we found that complete functional recovery was possible after 8 weeks of chronic IOP elevation, but no recovery was evident after 12 weeks of IOP elevation, although there was little evidence of any additional reduction in ganglion cell density.

Acknowledgments

Supported by Australian Research Council Future Fellowship.

Disclosure: **D. Zhao**, None; **V.H.Y. Wong**, None; **C.T.O. Nguyen**, None; **A.I. Jobling**, None; **E.L. Fletcher**, None; **A.J. Vingrys**, None; **B.V. Bui**, None

References

- Cook C, Foster P. Epidemiology of glaucoma: what's new? *Can J Ophthalmol*. 2012;47:223–226.
- Resnikoff S, Pascolini D, Etya'ale D, et al. Global data on visual impairment in the year 2002. *Bull World Health Organ*. 2004; 82:844–851.
- Asrani S, Zeimer R, Wilensky J, Gieser D, Vitale S, Lindenmuth K. Large diurnal fluctuations in intraocular pressure are an independent risk factor in patients with glaucoma. *J Glaucoma*. 2000;9:134–142.
- Leske MC, Wu SY, Hennis A, Honkanen R, Nemesure B; Barbados Eye Study Group. Risk factors for incident open-angle glaucoma: the Barbados Eye Studies. *Ophthalmology*. 2008;115:85–93.
- Anderson D, Drance SM, Schulzer M. The effectiveness of intraocular pressure reduction in the treatment of normal-tension glaucoma: Collaborative Normal-Tension Glaucoma Study Group. *Am J Ophthalmol*. 1998;126:498–505.
- Kim M, Kim DM, Park KH, Kim TW, Jeoung JW, Kim SH. Intraocular pressure reduction with topical medications and progression of normal-tension glaucoma: a 12-year mean follow-up study. *Acta Ophthalmol*. 2013;91:e270–e275.
- Leske MC, Heijl A, Hussein M, et al. Factors for glaucoma progression and the effect of treatment: the early manifest glaucoma trial. *Arch Ophthalmol*. 2003;121:48–56.
- Janz NK, Wren PA, Lichter PR, et al. The Collaborative Initial Glaucoma Treatment Study: interim quality of life findings after initial medical or surgical treatment of glaucoma. *Ophthalmology*. 2001;108:1954–1965.
- Lichter PR, Musch DC, Gillespie BW, et al. Interim clinical outcomes in the Collaborative Initial Glaucoma Treatment Study comparing initial treatment randomized to medications or surgery. *Ophthalmology*. 2001;108:1943–1953.
- Bowd C, Weinreb RN, Lee B, Emdadi A, Zangwill LM. Optic disk topography after medical treatment to reduce intraocular pressure. *Am J Ophthalmol*. 2000;130:280–286.
- Foulsham WS, Fu L, Tatham AJ. Visual improvement following glaucoma surgery: a case report. *BMC Ophthalmol*. 2014;14: 162.
- Ventura LM, Golubev I, Lee W, et al. Head-down posture induces PERG alterations in early glaucoma. *J Glaucoma*. 2013;22:255–264.
- Kong YX, Crowston JG, Vingrys AJ, Trounce IA, Bui VB. Functional changes in the retina during and after acute intraocular pressure elevation in mice. *Invest Ophthalmol Vis Sci*. 2009;50:5732–5740.
- Liu HH, He Z, Nguyen CT, Vingrys AJ, Bui BV. Reversal of functional loss in a rat model of chronic intraocular pressure elevation. *Ophthalmic Physiol Opt*. 2017;37:71–81.
- Sehi M, Grewal DS, Goodkin ML, Greenfield DS. Reversal of retinal ganglion cell dysfunction after surgical reduction of intraocular pressure. *Ophthalmology*. 2010;117:2329–2336.
- Ventura LM, Feuer WJ, Porciatti V. Progressive loss of retinal ganglion cell function is hindered with IOP-lowering treatment in early glaucoma. *Invest Ophthalmol Vis Sci*. 2012;53: 659–663.
- Anderson AJ, Stainer MJ. A control experiment for studies that show improved visual sensitivity with intraocular pressure lowering in glaucoma. *Ophthalmology*. 2014;121:2028–2032.
- Evans DW, Hosking SL, Gherghel D, Bartlett JD. Contrast sensitivity improves after brimonidine therapy in primary open angle glaucoma: a case for neuroprotection. *Br J Ophthalmol*. 2003;87:1463–1465.
- Gandolfi SA, Cimino L, Sangermani C, Ungaro N, Mora P, Tardini MG. Improvement of spatial contrast sensitivity threshold after surgical reduction of intraocular pressure in unilateral high-tension glaucoma. *Invest Ophthalmol Vis Sci*. 2005;46:197–201.
- He Z, Bui BV, Vingrys AJ. The rate of functional recovery from acute IOP elevation. *Invest Ophthalmol Vis Sci*. 2006;47: 4872–4880.
- El-Danaf RN, Huberman AD. Characteristic patterns of dendritic remodeling in early-stage glaucoma: evidence from genetically identified retinal ganglion cell types. *J Neurosci*. 2015;35:2329–2343.
- Guo L, Moss SE, Alexander RA, Ali RR, Fitzke FW, Cordeiro ME. Retinal ganglion cell apoptosis in glaucoma is related to intraocular pressure and IOP-induced effects on extracellular matrix. *Invest Ophthalmol Vis Sci*. 2005;46:175–182.
- Jones BW, Marc RE. Retinal remodeling during retinal degeneration. *Exp Eye Res*. 2005;81:123–137.
- Kim IJ, Zhang Y, Meister M, Sanes JR. Laminar restriction of retinal ganglion cell dendrites and axons: subtype-specific developmental patterns revealed with transgenic markers. *J Neurosci*. 2010;30:1452–1462.
- Liu HH, Bui BV, Nguyen CT, Kezic JM, Vingrys AJ, He Z. Chronic ocular hypertension induced by circumlimbal suture in rats. *Invest Ophthalmol Vis Sci*. 2015;56:2811–2820.
- Zhao D, Nguyen CT, Wong VH, et al. Characterization of the circumlimbal suture model of chronic IOP elevation in mice and assessment of changes in gene expression of stretch sensitive channels. *Front Neurosci*. 2017;11:41.
- Zhao D, He Z, Vingrys AJ, Bui BV, Nguyen CT. The effect of intraocular and intracranial pressure on retinal structure and function in rats. *Physiol Rep*. 2015;3:e12507.
- van Koeven AK, He Z, Nguyen CTO, Vingrys AJ, Bui BV. Systemic hypertension is not protective against chronic intraocular pressure elevation in a rodent model. *Sci Rep*. 2018;8:7107.
- Lamb TD, Pugh EN Jr. A quantitative account of the activation steps involved in phototransduction in amphibian photoreceptors. *J Physiol*. 1992;449:719–758.

30. Severns ML, Johnson MA. The care and fitting of Naka-Rushion functions to electroretinographic intensity-response data. *Doc Ophthalmol*. 1993;85:135-150.
31. Saszik SM, Robson JG, Frishman IJ. The scotopic threshold response of the dark-adapted electroretinogram of the mouse. *J Physiol*. 2002;543:899-916.
32. Naarendorp F, Sato Y, Cajdric A, Hubbard NP. Absolute and relative sensitivity of the scotopic system of rat: electroretinography and behavior. *Vis Neurosci*. 2001;18:641-656.
33. Bui BV, Fortune B. Ganglion cell contributions to the rat full-field electroretinogram. *J Physiol*. 2004;555:153-173.
34. Rodriguez AR, de Sevilla Muller LP, Brecha NC. The RNA binding protein RBPMS is a selective marker of ganglion cells in the mammalian retina. *J Comp Neurol*. 2014;522:1411-1443.
35. Liu HH, Flanagan JG. A mouse model of chronic ocular hypertension induced by circumlimbal suture. *Invest Ophthalmol Vis Sci*. 2017;58:353-361.
36. Morgan JE, Tribble JR. Microbead models in glaucoma. *Exp Eye Res*. 2015;141:9-14.
37. Urcola JH, Hernandez M, Vecino E. Three experimental glaucoma models in rats: comparison of the effects of intraocular pressure elevation on retinal ganglion cell size and death. *Exp Eye Res*. 2006;83:429-437.
38. Morrison JC, Cepurna WO, Johnson EC. Modeling glaucoma in rats by sclerosing aqueous outflow pathways to elevate intraocular pressure. *Exp Eye Res*. 2015;141:23-32.
39. Levkovitch-Verbin H, Quigley HA, Martin KR, Valenta D, Baumrind LA, Pease ME. Translimbal laser photocoagulation to the trabecular meshwork as a model of glaucoma in rats. *Invest Ophthalmol Vis Sci*. 2002;43:402-410.
40. Shareef SR, Garcia-Valenzuela E, Salierno A, Walsh J, Sharma SC. Chronic ocular hypertension following episcleral venous occlusion in rats. *Exp Eye Res*. 1995;61:379-382.
41. Livne-Bar I, Wei J, Liu HH, et al. Astrocyte-derived lipoxins A4 and B4 promote neuroprotection from acute and chronic injury. *J Clin Invest*. 2017;127:4403-4414.
42. Saleh M, Nagaraju M, Porciatti V. Longitudinal evaluation of retinal ganglion cell function and IOP in the DBA/2J mouse model of glaucoma. *Invest Ophthalmol Vis Sci*. 2007;48:4564-4572.
43. Rosch S, Johnen S, Muller F, Pfarrer C, Walter P. Correlations between ERG, OCT, and Anatomical Findings in the rd10 Mouse. *J Ophthalmol*. 2014;2014:874751.
44. de Hoz R, Ramirez AI, Gonzalez-Martin R, et al. Bilateral early activation of retinal microglial cells in a mouse model of unilateral laser-induced experimental ocular hypertension. *Exp Eye Res*. 2018;171:12-29.
45. Feng L, Chen H, Yi J, Troy JB, Zhang HF, Liu X. Long-term protection of retinal ganglion cells and visual function by brain-derived neurotrophic factor in mice with ocular hypertension. *Invest Ophthalmol Vis Sci*. 2016;57:3793-3802.
46. Mead B, Hill LJ, Blanch RJ, et al. Mesenchymal stromal cell-mediated neuroprotection and functional preservation of retinal ganglion cells in a rodent model of glaucoma. *Cytotherapy*. 2016;18:487-496.
47. Perez de Lara MJ, Santano C, Guzman-Aranguez A, et al. Assessment of inner retina dysfunction and progressive ganglion cell loss in a mouse model of glaucoma. *Exp Eye Res*. 2014;122:40-49.
48. Kong YX, van Bergen N, Bui BV, et al. Impact of aging and diet restriction on retinal function during and after acute intraocular pressure injury. *Neurobiol Aging*. 2012;33:1126e1115.
49. Nguyen CT, Vingrys AJ, Wong VH, Bui BV. Identifying cell class specific losses from serially generated electroretinogram components. *Biomed Res Int*. 2013;2013:796362.
50. Weitlauf C, Ward NJ, Lambert WS, et al. Short-term increases in transient receptor potential vanilloid-1 mediate stress-induced enhancement of neuronal excitation. *J Neurosci*. 2014;34:15369-15381.
51. Sappington RM, Sidorova T, Ward NJ, Chakravarthy R, Ho KW, Calkins DJ. Activation of transient receptor potential vanilloid-1 (TRPV1) influences how retinal ganglion cell neurons respond to pressure-related stress. *Channels (Austin)*. 2015;9:102-113.
52. Ryskamp DA, Witkovsky P, Barabas P, et al. The polymodal ion channel transient receptor potential vanilloid 4 modulates calcium flux, spiking rate, and apoptosis of mouse retinal ganglion cells. *J Neurosci*. 2011;31:7089-7101.
53. Puthussery T, Yee P, Vingrys AJ, Fletcher EL. Evidence for the involvement of purinergic P2X receptors in outer retinal processing. *Eur J Neurosci*. 2006;24:7-19.
54. Vessey KA, Fletcher EL. Rod and cone pathway signalling is altered in the P2X7 receptor knock out mouse. *PLoS One*. 2012;7:e29990.